Pharm Res (2011) 28:107–116
DOI 10.1007/s11095-010-0123-9

RESEARCH PAPER

Microneedle-Based Intradermal Delivery Enables Rapid Lymphatic Uptake and Distribution of Protein Drugs

Alfred J. Harvey • Scott A. Kaestner • Diane E. Sutter • Noel G. Harvey • John A. Mikszta • Ronald J. Pettis

Received: 30 November 2009 / Accepted: 8 March 2010 / Published online: 31 March 2010

ABSTRACT

Purpose The purpose of this research was to examine the pharmacokinetics (PK) of drug uptake for microneedle-based intradermal (ID) delivery of several classes of protein drugs compared to standard subcutaneous (SC) administration.

Methods Systemic absorption kinetics of various proteins were analyzed following microneedle-based ID delivery and standard injection methods in the swine model. Comparative PK data were determined using standard non-compartmental techniques based on blood serum levels.

Results Delivery of proteins using microneedles resulted in faster systemic availability, measured via $t_{max,}$ and increased maximal drug concentration, $C_{max,}$ over SC delivery for all proteins tested. Some agents also exhibited increased bioavailability for the ID route. Imaging studies using reporter dyes showed rapid lymphatic-mediated uptake.

Conclusions Microneedle delivery is applicable to a wide variety of protein drugs and is capable of effective parenteral administration of therapeutic drug dosages. This delivery route alters absorption kinetics via targeting a tissue bed better perfused with lymphatic and blood vessels than the SC space. Microneedle delivery may afford various advantages, including a robust method to increase the absorption rate and bioavailability of proteins that have been challenging to deliver at therapeutic levels or with physiologically relevant profiles.

KEY WORDS insulin · intradermal delivery · lymphatic uptake · microneedle · pharmacodynamics · pharmacokinetics · protein

A. J. Harvey · S. A. Kaestner · D. E. Sutter · N. G. Harvey · J. A. Mikszta · R. J. Pettis (✉)
BD Technologies,
21 Davis Drive,
Research Triangle Park, North Carolina 27709, USA
e-mail: rpettis@bd.com

ABBREVIATIONS

AAALAC	Association for Assessment and Accreditation of Laboratory Animal Care
BG	Blood glucose
C_{max}	Maximum blood concentration
IACUC	Institutional Animal Care and Use Committee
ICG	Intracardiac green dye
ID	Intradermal
IM	Intramuscular
IV	Intravenous
NIH	National Institutes of Health
NIR	Near infrared
PD	Pharmacodynamics
PK	Pharmacokinetics
rhGH	Recombinant human growth hormone
SC	Subcutaneous
SD	Standard deviation
SEM	Standard error of the mean
SWFI	Sterile water for injection
$t1/2_{\lambda z}$	Terminal half life
TB	Tuberculosis
t_{max}	Time to max blood concentration
TNFα	Tumor necrosis factor alpha
USDA	United States Department of Agriculture
VAP	Vascular access port

INTRODUCTION

The development and use of peptide and protein therapeutic drugs is increasing, and their administration continues to rely on standard parenteral injection techniques (1–3). Alternative delivery methods, such as transdermal delivery, are typically limited by diffusion through the stratum corneum of the skin (4). While disruption of the stratum corneum with solid or

hollow glass microneedles or other means can enhance total transport, the total delivered doses and fluid volumes remain small and often require significant time, potentially limiting the applicability of this pathway (5,6). Other alternative routes, such as inhalation (7,8) and nasal (9) delivery, similarly suffer from low bioavailability and concerns regarding dose accuracy, reproducibility and chronic exposure. Similarly, some protein drugs, such as many endocrine hormones, require uptake tailored to mimic complex native secretion profiles to achieve maximal therapeutic response (10,11). Intravenous (IV) injection maximizes both bioavailability and the ability to manipulate dosing profiles but is not practical for self-administration due to the complexity and risks of initiating and maintaining venous access (12,13). Subcutaneous (SC) injection is often the preferred delivery route, but this method suffers from user preference and compliance issues, sluggish or variable absorption kinetics, and sometimes limited bioavailability (14,15). The high molecular weight of many therapeutic antibodies and proteins may further complicate these issues.

Conversely, hollow steel microneedles provide a parenteral delivery technique combining many of the reliability and ease-of-use aspects of traditional injection in a minimally invasive system. Although there are no universally recognized dimensions for microneedles, for these studies, we define them as hollow cannula with total lengths of 2 mm or less for tissue insertion and individual external lumen diameters of no more than 300 μm. Microneedles are applicable to a broad range of agents and have demonstrated excellent reliability for clinical dosing (16). Microneedle devices have been designed to link to common drug reservoirs using standardized luer connections, and to mimic current injection practices (17,18). Compared to silicon (19) or glass (20) microneedles, steel is more mechanically robust, has good manufacturability and is easily integrated into delivery systems. Steel needles also have well-known toxicological properties with recognized drug and tissue compatibility, which has not yet been widely demonstrated for alternative microneedle materials. Stainless steel microneedles are capable of delivering clinically meaningful doses, both volumetrically and on a mass basis. We have previously used microneedles to administer numerous vaccines in pre-clinical models (21–26), and these devices have also progressed through Phase I–III clinical trials for influenza vaccines (27–30) with product licensure obtained in Europe (31).

Lastly, microneedles access a unique tissue bed: the viable dermis. The uptake properties from this tissue after direct intradermal (ID) administration have not been well studied, especially for proteins and peptides, principally due to the difficulty of directly and reliably accessing this tissue bed by mechanical means (32,33). Historical methods of ID access, such as the Mantoux method used for tuberculosis (TB) skin testing, have utilized device systems inappropriately scaled to the dimensions of the target tissue bed. Similarly, this method has suffered from a high degree of user variability (16) and has classically been used for vaccines where systemic absorption is not traditionally studied. The dermis is more highly perfused with vascular and lymph capillary networks. The regional capillaries and lymph vessels have reduced barrier properties to absorption due to their reduced wall thickness and endothelial barrier (34–36). The dermis is also a very active tissue from both a cellular turnover and immunological perspective (37,38). It is reasonable to believe that the ID route may have unique pharmacokinetic (PK) properties compared to other parenteral routes, such as IV, SC and intramuscular (IM), based on these physiological differences.

In this paper, we examine the pharmacokinetics and pharmacodynamics (PD) for various protein drugs after parenteral administration directly into the viable dermal bed using stainless steel microneedles. We have explored drug uptake across a range of different drug classes and molecular weights and have utilized a large mammalian animal model to increase the relevance to human dosing. Here we report on the unique PK profiles obtained and the excellent mechanical reliability for drug deposition using microneedle-based ID delivery.

MATERIALS AND METHODS

Microneedle Delivery Devices

Steel microcannula were manually assembled into catheter-based devices for fluid administration to the ID space. All microcannula were 34 gauge steel stock (176 micron nominal outer diameter) with a single 28° bevel and a total tissue penetration length of 1.0 mm (Fig. 1). Microneedle catheters consisted of flexible tubing with a luer connection and were attached to an analytical microsyringe drug reservoir (Hamilton Gas-tight, Hamilton Company, Reno, NV). For indocyanine green imaging, insulin, and somatropin studies, single microneedle devices were used. Due to the increased viscosity and dosing volume for etanercept, a microneedle array containing three microcannula incorporated into a fluid-distributing hub was used. All microdevices were primed, and fluid flow was confirmed both immediately prior to and post injection. A sham injection with subsequent content analysis was performed under the specific dosing conditions for each drug to confirm that no protein degradation was induced by passage through the microneedles (data not shown).

During injection, microneedles were inserted perpendicular to the skin surface on the animal's flank and held in place with medical adhesive for the duration of injection.

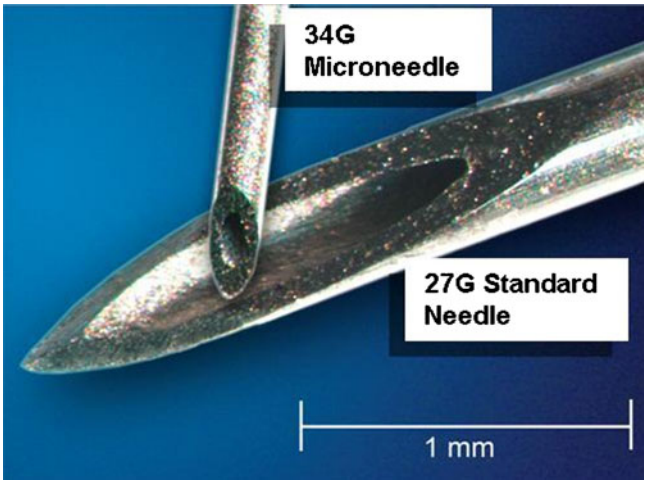

Fig. 1 Micrograph showing a 34G microneedle and a standard 27G needle. A microneedle's smaller diameter and shorter bevel are better suited for reliably targeting compounds to the ID space without fluid leakage.

Drug delivery rate and volume for all microneedle injections was controlled using a syringe pump (Harvard PHD 2000, Harvard Apparatus, Holliston, MA). Delivery volume was visually confirmed after injection using the syringe barrel graduations. Any drug leakage to the skin surface was quantified gravimetrically using a previously validated method (39). Any doses exhibiting greater than 5% leakage by volume were excluded from PK analysis. IV dosing was accomplished via a marginal ear vein catheter (Insyte®, BD, Franklin Lakes, NJ). SC injections were performed in the flank using a standard 27G needle (BD) in the same region as ID administration to reduce the potential for site-related variation in uptake. Injection rates for SC and IV injections were manually controlled rapid bolus pushes of approximately 5–10 s duration.

In Vivo Models

Near-infrared (NIR) imaging studies were performed on 25–35 kg female Yorkshire swine (Archer Farms, Darlington, MD). All PK studies were performed on Yucatan mini pigs in a 20–30 kg weight-range (Sinclair Research Center, Columbia, Missouri) with surgically implanted vascular access ports (VAP). Swine used for insulin studies were rendered diabetic by prior injection of streptozotocin following published methods (40). Animals were temporarily sedated during drug dosing and VAP prep, and access by injection of a tiletamine/zolazepam/xylazine/atropine anesthetic cocktail, recovered, and transferred to individual caging for the duration of the study. A replicate of at least five animals was performed for all studies. Where possible, dosing for each agent was performed in a single animal cohort using a randomized full cross-over study design with each animal serving as its own control for each delivery route. Similarly, all dosing was conducted in as short a time as possible, typically 2 weeks, to reduce the immunogenicity potential against recombinant human or humanized proteins. All *in vivo* work was performed under approved IACUC protocols in an AAALAC accredited facility following USDA and NIH guidelines, and adhered to the "Principles of Laboratory Animal Care" (NIH publication #85-23, revised 1985.)

Drug Dosing, Sample Analysis, and PK

Etanercept

Etanercept (Enbrel®, Immunex, Seattle, WA) was provided as a concentrated liquid formulation of 80 mg/ml at pH 6.2 and used as supplied. The drug solution was aliquoted, stored frozen at −70°C, and equilibrated to room temperature just prior to administration. Due to the extended drug half-life, a non-crossover dosing design was employed, with each animal (n=6/route) receiving a single 250 μl (20 mg) injection at a rate of 20 μl/min by either the microneedle ID, SC, or IV route. Blood samples were drawn at t=0, 0.5, 1, 1.5, 2, 3, 4, 6, 8, 12, 24, 36, 72, 96, 144, 192, and 240 h after administration into Vacutainer® serum tubes (BD, Sparks, MD), allowed to clot at room temperature, centrifugally separated, and stored in cryotubes at −70°C until analysis. Equivalent serum sample prep was used for other agents. Quantitative analysis was via a proprietary ELISA methodology, with a lower limit of quantitation of 0.3 ng/ml. Naive mini-pig swine serum was prescreened to confirm the absence of assay interference. Noncompartmental PK analysis was performed on both individual and mean concentration-time profiles. Statistical significance was determined by the Wilcoxon test for differences in medians, with 95% confidence intervals determined by the Hodges-Lehman procedure.

Somatropin

Somatropin, recombinant human growth hormone (rhGH) (Genotropin™, Pharmacia, Kalamazoo, MI) was received as a lyophilized powder and reconstituted using sterile water for injection (SWFI) containing sufficient mannitol for isotonicity at a nominal concentration of 36 IU/ml immediately prior to injection. A full crossover study design (n=8/route) was utilized with a minimum two-day washout period between doses. Each dose was standardized to 100 μl volume, containing 3.6 IU rhGH. Microneedle delivery rate was 45 μl/min with a 2.2 min infusion duration. Blood sampling times began at injection completion at t=0, 0.25, 0.5, 1, 1.5, 2, 3, 5, 8, 10, 14, 24, and 30 h

(ID and SC) or 0, 5, 10, 15, 20, 30, 45, 60, 90, 120, 180, and 360 min (IV). After clotting, serum was assayed for rhGH content using a commercial DELFIA® hGH Assay Kit (Wallac Oy, Oulunsalo, Finland) and analyzed on a Victor 1420 time-resolved fluorometer (PerkinElmer Inc., Gaithersburg, MD). PK analysis was performed using WinNonLin 2.1 noncompartmental analysis, with doses normalized for body weight. Statistical analysis was performed in MiniTab 15 using a standard paired *t*-test.

Insulin

Recombinant regular human insulin (Hoechst-Roussel, Somerville, NJ) and the rapid-acting analog, insulin lispro (Humalog®, Eli Lilly, Indianapolis, IN), were used as purchased from a retail pharmacy and maintained under refrigerated conditions between use. Insulin concentration was U100 (100 IU/ml) for both insulin types, with an administered dose of 5 IU per animal (50 µl by volume). A partial crossover study design was utilized (n=5–9/condition). Insulin lispro was administered both ID (100 uL/min rate) and SC, while regular insulin was administered ID only. Sampling times were 0, 5, 10, 15, 20, 30, 40, 50, 60, 75, 90, 120, 150, 180, 240, 300 min post injection. Blood glucose (BG) levels were checked at concomitant times using commercial glucose oxidase strips for venous blood and handheld glucometers (Accu-Check®, Roche Diagnostics, Indianapolis, IN) with daily reference checks performed per manufacturer's instructions. Animals having low BG values (<20 mg/dl) or showing physical signs of hypoglycemia were administered IV glucose, and their PD profiles were curtailed at that time, with subsequent BG checks performed for safety purposes only. Insulin content was analyzed using a commercial chemiluminescent immunoassay (DPC, Los Angeles, CA) on a clinical lab analyzer (Immulite, DPC Cirrus Inc, Flanders, NJ), with confirmed cross-reactivity for both insulin types. Non-compartmental PK analysis was performed using WinNonLin Version 3.2. Statistical analysis was performed using Tukey 95% simultaneous confidence intervals for pairwise comparisons.

Indocyanine Green Imaging

Indocyanine Green (ICG) (Cardiogreen, Sigma-Aldrich, St. Louis, MO) was diluted to 200 µM with sterile water just prior to use. ID administration of ICG was performed on the abdomen of the swine in a 200 µl volume, at a delivery rate of 100 µl/min. Excitation illumination was created using 750 nm filter sets (Omega Optical, Brattleboro, VT) over halogen lamps. Emission wavelength was collected using a 790 nm filter (Omega Optical) over the video camera (EXvision, SuperCircuits, Austin, TX) lens. Still images were extracted from the time-course video at specific time points.

RESULTS

To examine the effect of microneedle-based ID delivery on drug uptake, we generated PK profiles in swine for four drugs of varying biochemical characteristics and physiological activity: etanercept, a 132 kD TNFα-binding, recombinant dimeric fusion protein for the treatment of rheumatoid arthritis; somatropin, a 22 kD endocrine hormone for treatment of growth disorders; regular recombinant human insulin, a 5.8 kD pancreatic protein for the treatment of diabetes which typically exists as a hexamer of 35 kD; and insulin lispro, a rapid-acting insulin analog existing principally in dimeric form at 11.6 kD.

Based on the PK determinations for the various protein drugs tested, it is clear that microneedle-based ID administration creates a unique PK profile not anticipated by either previous work in the transdermal field, nor from historical parenteral studies including SC and skin-targeting injections using conventional needles or other means. The hallmark feature for the microneedle route in all cases is the extremely rapid uptake and systemic distribution from the injection site when compared to SC administration (Figs. 2, 3 and 4). For each protein studied, the time to maximum concentration (t_{max}), was significantly reduced: 71% for etanercept, 83% for somatropin, and 64% for insulin lispro. The percentage change for regular insulin was not determined due to the lack of SC regular arm in this study. However, in a similar diabetic mini-pig model (40), the reported t_{max} was 100 min for SC regular, which would represent a 77% decrease in peak onset time for the ID route.

As a result of the rapid uptake, maximum circulating peak concentrations were also routinely elevated several

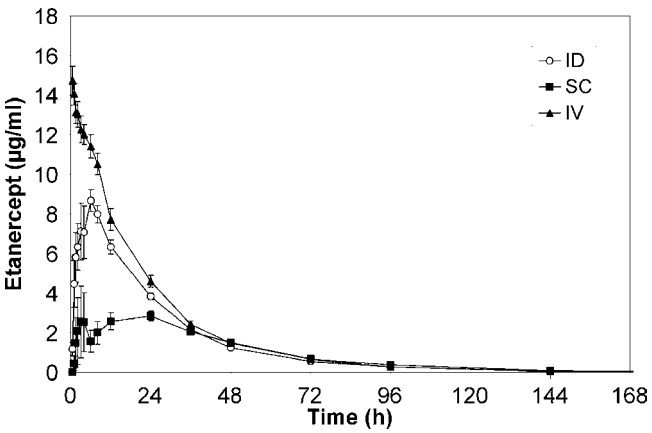

Fig. 2 Average PK profiles in swine (n=6, ±SEM) following ID, SC, and IV injections of 20 mg etanercept.

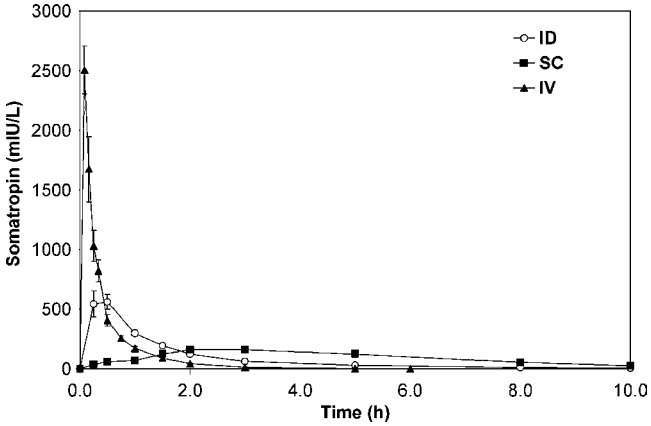

Fig. 3 Average PK profiles in swine ($n = 8$, ±SEM) following ID, SC, and IV injections of 3.6 IU somatropin.

fold compared to SC delivery: 193% increase for etanercept, 386% for somatropin, and 349% for insulin lispro. This effect on maximal blood concentration was also compounded by an increase in bioavailability observed for some agents. For etanercept, the mean absolute bioavailability (*vs.* IV) was 75%, which correlated to a 50% increase in relative bioavailability *vs.* SC (Table I). Bioavailability for somatropin was essentially 100% for all administration routes tested, with no significant differences between routes (Table II). For insulin lispro, microneedle delivery exhibited a 19% increase in absolute bioavailability (IV data not shown) and 40% increase in relative bioavailability; however, the differences were not statistically significant (Table III). Bioavailability for regular insulin could not be determined without an IV control arm. Interestingly, both insulin types, regular and rapid-analog, despite their differences in molecular weight, exhibited almost identical PK outcomes in the diabetic swine model used for testing (Fig. 4A). Notably, both insulin types delivered by microneedle showed more rapid onset than SC delivery of insulin lispro.

For insulin delivery in diabetic swine, PD responsiveness was also measured (Fig. 4B). Decrease of the blood glucose (BG) values was detectable in most microneedle-dosed animals within 5 min post-dosing, again regardless of insulin type. SC injection typically required 15 min or longer for observable changes. Similarly, the rate of BG decline was faster in microneedle cohorts. Differences in maximal BG reduction between arms could not be determined because almost all animals required rescue glucose to prevent hypoglycemia complications, and PD data after glucose rescue were not collected. However, mean BG levels for the ID doses were below SC for most time points out to 60 min.

Drug doses in these studies ranged from 227.5 μg to 20 mg of active agents with volumes ranging from 0.05 ml to 0.25 ml. No damage, bending or breakage of the steel microcannula was observed during use, and volumetric accuracy was good in all cases without discernable leakage. The various flow rates utilized were chosen to ensure dose accuracy for the formulation and delivery volume of the specific study, while maintaining a uniform delivery period necessary for consistent PK sampling. Specific infusion pressures were an uncontrolled factor in these studies. However, in related microneedle experiments, equivalent insulin doses (10 IU) administered ID using variable drug concentrations at delivery volumes from 50 to 250 uL yielded equivalent pharmacokinetic outcomes (data not shown), even though the tissue pressure of injection may have varied. Likewise, local tissue reactions typically consisted of minor edema formation at the local injection site which typically resolved within 1–2 h after injection. Site reactions following ID etanercept injections were longer, requiring 12 h to resolve, and correlated with the

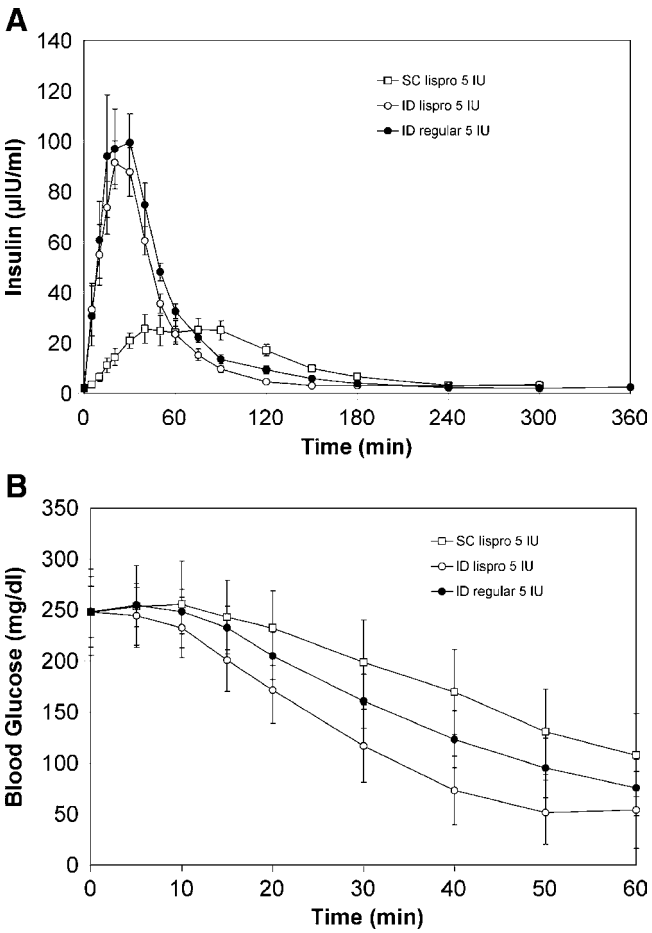

Fig. 4 **A** Average PK profiles in swine ($n = 5$–8, ±SEM) following ID, and SC injection of 5 IU rapid analog insulin lispro and ID injection of 5 IU regular recombinant human insulin. ID injection shows rapid uptake with little discrimination between insulin types. **B** Average corresponding PD profiles for the insulin PK curves in (**A**). Average BG starting values were normalized to 250 mg/dl. ID delivery exhibits more rapid decline and lower average blood glucose levels at 60 min compared to SC delivery of rapid insulin.

Table I Summary of Non-compartmental Analysis of Etanercept PK Parameters

ETANERCEPT		IV	ID	SC
t_{max}	hr	0.43 ± 0.79	5.21 ± 2.20[a]	17.80 ± 9.7
C_{max}	ng/ml	16,545 ± 2,363	9,002 ± 1,884[a]	4,657 ± 3,375
$t1/2_{\lambda z}$	hr	16.9 ± 1.0	17.8 ± 1.1[a]	24.8 ± 4.6
AUC(∞)	ng·hr/ml	319,522 ± 41,323	239,765 ± 34,753[a]	158,759 ± 13,670
% Bioavailabilty	AUC/IV AUC	100	75[a]	50

[a] Indicates statistical significance compared to SC, $p < 0.05$

observed t_{max} value for this drug. However, injection site reaction is also a common side effect for etanercept when used subcutaneously.

To examine the mechanism associated with the more rapid uptake of protein drugs following microneedle delivery, we performed imaging studies with a NIR fluorescent dye, ICG. ID delivery of ICG resulted in immediate uptake by the local lymphatic vessels as shown in Fig. 5. The draining inguinal lymph node could easily be identified within 20 s and continued to increase in signal strength through the 3-min observation period. The draining lymph node was approximately 40 cm from the injection site. No lymphatic uptake was seen within the observation period from corresponding SC injections; instead, fluorescence remained principally localized at the injection site. Conversely, IV injection of an equivalent dose resulted in essentially instantaneous illumination of all peripheral vasculature, but without detectable visible localization in the lymph node. Although these peripheral vessels were not illuminated during ID injection, we cannot rule out a potential contribution from venous capillary uptake of ICG, a low molecular weight dye (MWt = 775 Da) that may have been below the limits of our through-skin visual detection (data not shown). These results suggest that rapid lymphatic uptake may contribute, at least in part, to the rapid PK and PD effects seen *versus* standard SC injection.

DISCUSSION

The dramatic differences seen from the microneedle dosing are counterintuitive to those expected for classical transdermal delivery. In those cases, the stratum corneum provides an almost impermeable barrier to transport of hydrophilic macromolecular drugs (41). Puncture of the stratum corneum by solid microneedles increases diffusional transport (42); however, the total mass of administered drug and the extended times required for delivery may limit the potential applicability of this pathway for many drug delivery applications. Likewise, while subcutaneous injection is one of the most commonly used forms of parenteral delivery, uptake of drugs from this tissue can be slow and can vary substantially based on factors such as injection technique (43) and body mass index (44). Similarly, for many protein therapeutics, especially hormone replacement therapies, slow SC absorption is often cited as limiting for obtaining effective therapeutic endpoints. This is especially true for insulin, where substantial effort has been expended on the development of insulin analogs to better mimic the rapid first-phase pancreatic response which occurs after eating. To date, none of these agents has yet to achieve the 10–15 min onset kinetics of native insulin secretion. Similarly, human growth hormone is naturally delivered in periodic pulses, and these temporal fluctuations are beneficial for its physiological activity (45). The need to better imitate this native profile to maximize therapeutic responsiveness continues to be intensely investigated (46).

Parenteral delivery of many proteins has reduced or limited bioavailability for non-IV delivery routes. This can require the administration of excess drug to reach therapeutic levels. In contrast, for the various proteins examined, microneedle delivery exhibited very high bioavailability. For the recombinant TNFα binding chimeric protein, etanercept, microneedle administration demonstrated substantially higher bioavailability than the traditional SC

Table II Summary of Non-compartmental Analysis of Somatropin PK Parameters

SOMATROPIN		IV	ID	SC
t_{max}	hr	0.09 ± 0.05	0.47 ± 0.25[a]	2.75 ± 0.46
C_{max}	mIU/ml	2,860.00 ± 1,599.10	612.60 ± 187.10[a]	158.50 ± 31.00
$t1/2_{\lambda z}$	hr	0.66 ± 0.10	2.02 ± 0.448[a]	1.19 ± 0.49
AUC(∞)	mIU·hr/ml	844.50 ± 249.70	850.00 ± 170.00	920.20 ± 251.70
% Bioavailability	AUC/IV AUC	100	101	109

[a] Indicates statistical significance compared to SC, $p < 0.05$

Table III Summary of Non-compartmental Analysis of Insulin PK Parameters

INSULIN		SC - lispro	ID - lispro	ID - Regular
t_{max}	min	61.00 ± 20.74	21.875 ± 7.53[a]	25.00 ± 6.45[a]
C_{max}	μIU/ml	31.76 ± 10.58	107.47 ± 26.81[a]	117.51 ± 56.01[a]
$t1/2_{\lambda z}$	min	62.87 ± 33.22	41.54 ± 29.06	47.65 ± 22.96
AUC(∞)	mIU·min/ml	3,720.11 ± 753.26	4,780.84 ± 1,112.37	5,738.51 ± 1,674.41
% Bioavailability	AUC/IV lispro AUC	48	67	n/a

[a] Indicates statistical significance compared to SC, $p < 0.05$

route. Similarly, other reported microneedle studies have reported delivery of modest volumes of insulin and other drugs. In this study, human therapeutic levels of various agents were consistently delivered in timeframes meaningful for therapeutic intervention.

The unique PK observed for microneedle delivery in all cases implies an uptake mechanism unlike that expected for either traditional transdermal, intradermal, or subcutaneous delivery. As demonstrated by the NIR imaging studies with ICG dye, lymphatic absorption may be a significant contributor of uptake from microneedle delivery. The contribution of lymphatic absorption on insulin and other macromolecule uptake has been previously evaluated. In those studies, the role of the lymphatics in SC uptake was limited (47) and highly dependent on the choice of animal model (48), drug molecular weight, and formulation (49) employed. The extremely rapid absorption observed in microneedle imaging and PK studies, however, does not agree well with typical estimates of slow basal lymphatic flow. In related work using these microdevices in preclinical swine models (50) and breast cancer patients undergoing lymph node imaging and resection (51), lymph flow following microneedle delivery

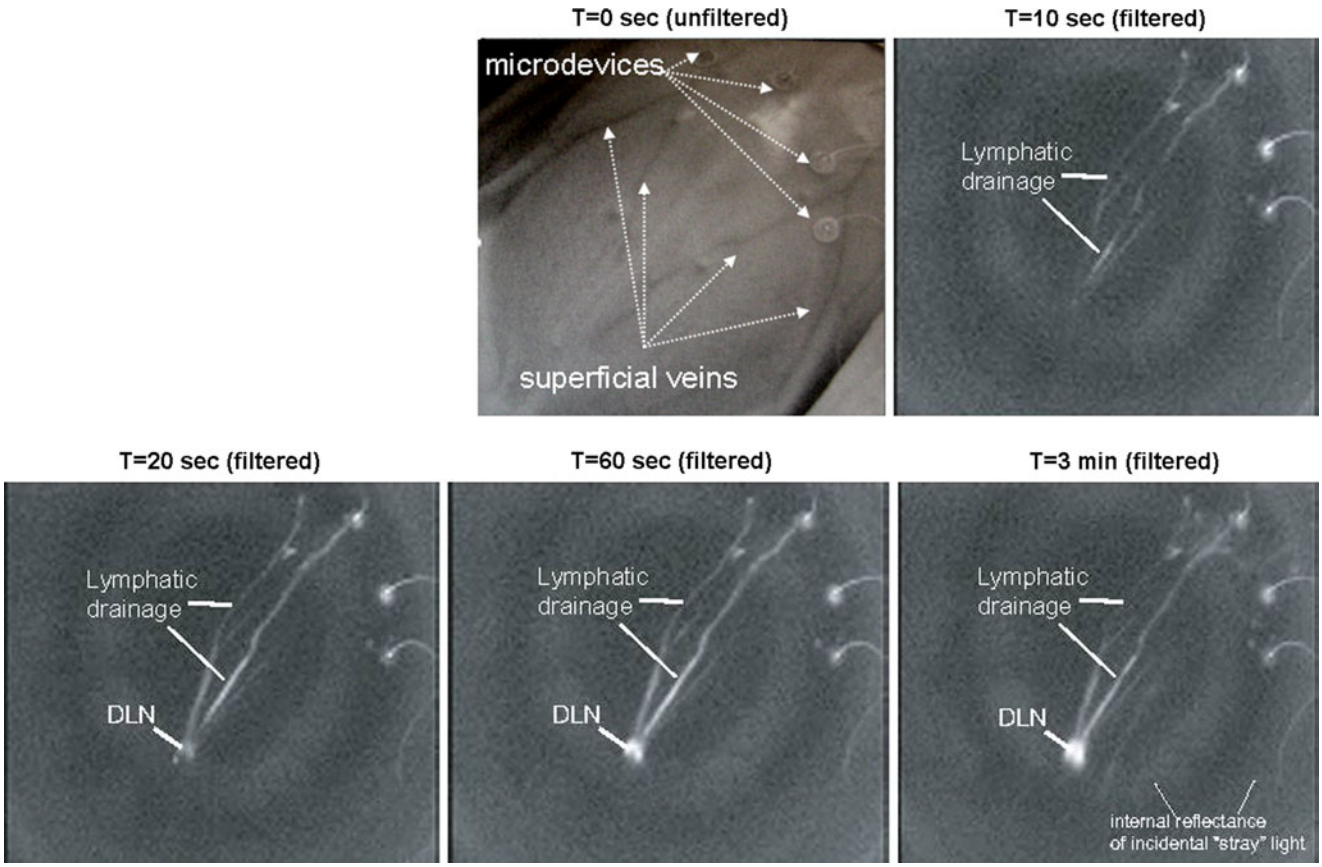

Fig. 5 Time-course of NIR fluorescent imaging through intact skin of two simultaneous ID ICG injections in the abdomen of the swine. A total of four microneedle catheter devices (seen in the white light T = 0 image) were placed on the animal; however, injections were only performed through the upper two devices in the image frame. Instantaneous draining of the injection sites occurs via the regional lymph vessels with increasing fluorescence detectable in the draining lymph nodes over time.

was measured to be 1,000-fold faster than under previously determined physiologic conditions.

This concept of lymph-driven uptake is also supported by the PK similarities observed between regular and analog insulin that differ in molecular weights (MWt) by 3-fold. Historically, insulin absorption from the SC space has been thought to occur via venous microcapillary absorption and then only for insulin monomers and dimers following dissociation from higher multimeric states (52). Since the lymphatics have reduced endothelial barrier properties and direct ID deposition via microneedles limits the required diffusion through the SC matrix, a lymph-mediated absorption route seems plausible. Once absorption occurs and agents are delivered into systemic circulation, there appears to be no apparent difference in terminal clearance, as indicated by similar t1/2 λz values to SC, although most drugs show a faster return to baseline levels due to the faster absorption. This again implies a PK mechanism based on faster uptake rather than differences in terminal metabolism and clearance.

Obviously, these unique PK effects may not be optimal for all compounds. However, in the case of insulin, microneedle delivery offers kinetics that are currently unattainable from SC delivery of rapid-acting insulin analogs and are considerably closer to the insulin release from healthy pancreatic beta cells. This rapid uptake may allow better post-prandial glucose control by speeding the onset of insulin metabolic activity, while the faster offset also seen with ID delivery could have implications for reduction of hypoglycemia. ID delivery of pain relief compounds is another example of agents that could benefit from this more rapid PK profile. The potential effects of high level or repetitive exposure of protein drugs on the lymphatics and immune system have not been fully investigated. Further evaluation with specific compounds is warranted, especially in cases of chronic therapies. However, this unique lymphatic targeting could also demonstrate additional benefit for drugs that are intended to specifically target the immune system, such as vaccines, certain cancer therapies and immunomodulators.

Although a full crossover of devices, i.e. using different needle gauges to deposit either ID or SC, was not tested for all compounds, a study examining SC delivery of insulin through longer microneedles (3 mm) showed no PK/PD differences when compared to SC injection with a standard gauge needle (data not shown). Also, ID injections with a 27 g needle were not compared due to the difficulty of reliably and accurately targeting the ID space with a standard needle (39), and historical precedents did not show significant PK differences using ID injection methods with standard gauge needles (33). The pressure required to inject ID is higher than that for the SC space due to both the reduced cross-sectional area of the microneedle fluid path and the increased density and collagen structure of the dermal tissue. It has been demonstrated that increasing dermal pressure increases lymphatic system fluid absorption (53). The effective ID localization of the injection volume combined with the increased interstitial pressure, may contribute to the lymphatic absorption seen with microneedle delivery.

An effective translation of microneedles into the clinical setting is ultimately necessary to realize their potential therapy benefits. Similar microneedles to those in this study have been used in numerous preclinical and clinical studies for delivery of various drug and vaccine compounds (21–30). These studies have shown that microneedles allow for more reliable and reproducible access to the dermal tissue than standard needles (39). A commercial prefilled microneedle product (Soluvia™, BD) for delivery of intradermal influenza vaccine (Intanza®/ID Flu®, sanofi-pasteur), has received regulatory approval in Europe, and others are in development.

CONCLUSIONS

Overall, microneedle-based ID delivery demonstrates numerous potential benefits for parenteral protein delivery. This methodology has demonstrated broad applicability to a range of protein therapeutic molecular weights and therapeutic classes, with no deleterious effects on drug stability due to shear degradation. The devices themselves exhibited no damage during use and were capable of accurately and reproducibly delivering volumetric doses between 50 and 250 uL, in brief timeframes. Total drug dosing was consistent with the ranges required for human therapeutic use. No changes or only a minor concentration of the etanercept formulation were required to achieve therapeutic doses while remaining within the volumetric limitations of microneedle delivery. Lastly, the microneedle devices appear to enable a unique uptake mechanism allowing distinct PK parameters not achieved with other injection methods. Among these are rapid uptake, increased C_{max}, and, in some cases, increased bioavailability or reduced circulating lifetimes. These properties may provide additional benefit for some therapy regimens, such as hormone replacement and pain management, where rapid PK is beneficial, or in cases where direct lymphatic targeting would be valuable, such as in cancer treatment, immunomodulation therapies, and diagnostic imaging.

ACKNOWLEDGEMENTS

This work was funded by BD. We wish to thank Immunex and Pharmacia for providing etanercept and rhGH, respectively, PK support, and partial funding. From BD Technologies, Steven Keith for his PK work on insulin, Colleen Nycz for her

work with lymphatic imaging, and Tommy Robinson, Frank Martin, and Scott O'Connor for their microdevice manufacturing effort are also gratefully acknowledged.

REFERENCES

1. Kang JS, Deluca PP, Lee KC. Emerging PEGylated drugs. Expert Opin Emerg Drugs. 2009;14(2):363–80.
2. Nieri P, Donadio E, Rossi S, Adinolfi B, Podestà A. Antibodies for therapeutic uses and the evolution of biotechniques. Curr Med Chem. 2009;16(6):753–79.
3. Wurch T, Lowe P, Caussanel V, Bes C, Beck A, Corvaia N. Development of novel protein scaffolds as alternatives to whole antibodies for imaging and therapy: status on discovery research and clinical validation. Curr Pharm Biotechnol. 2008;9(6):502–9.
4. Simon L, Goyal A. Dynamics and control of percutaneous drug absorption in the presence of epidermal turnover. J Pharm Sci. 2009;98(1):187–204.
5. Martanto W, Moore JS, Couse T, Prausnitz MR. Mechanism of fluid infusion during microneedle insertion and retraction. J Control Release. 2006;112(3):357–61.
6. Prausnitz MR. Microneedles for transdermal drug delivery. Adv Drug Deliv Rev. 2004;56(5):581–7.
7. Garg SK, Mathieu C, Rais N, Gao H, Tobian JA, Gates JR *et al.* Two-year efficacy and safety of AIR inhaled insulin in patients with type 1 diabetes: an open-label randomized controlled trial. Diabetes Technol Ther. 2009;11 Suppl 2:S5–S16.
8. Shoyele SA, Slowey A. Prospects of formulating proteins/peptides as aerosols for pulmonary drug delivery. Int J Pharm. 2006;314(1):1–8.
9. Costantino HR, Illum L, Brandt G, Johnson PH, Quay SC. Intranasal delivery: physicochemical and therapeutic aspects. Int J Pharm. 2007;337(1–2):1–24.
10. Haus E. Chronobiology in the endocrine system. Adv Drug Deliv Rev. 2007;59(9–10):985–1014.
11. Guerci B, Sauvanet JP. Subcutaneous insulin: pharmacokinetic variability and glycemic variability. Diabetes Metab. 2005;31(4 Part 2):4S7–4S24.
12. Hamilton H. Complications associated with venous access devices: part one. Nurs Stand. 2006;20(41):67.
13. Hamilton H. Complications associated with venous access devices: part two. Nurs Stand. 2006;20(27):59–65.
14. Brunton S. Insulin delivery systems: reducing barriers to insulin therapy and advancing diabetes mellitus treatment. Am J Med. 2008;121(6 Suppl):S35–41.
15. Gin H, Hanaire-Broutin H. Reproducibility and variability in the action of injected insulin. Diabetes Metab. 2005;31(1):7–13.
16. Laurent PE, Bonnet S, Alchas P, Regolini P, Mikszta JA, Pettis R *et al.* Evaluation of the clinical performance of a new intradermal vaccine administration technique and associated delivery system. Vaccine. 2007;25(52):8833–42.
17. Mikszta JA, Laurent PE. Cutaneous delivery of prophylactic and therapeutic vaccines: historical perspective and future outlook. Expert Rev Vaccines. 2008;7(9):1329–39.
18. Lambert PH, Laurent PE. Intradermal vaccine delivery: will new delivery systems transform vaccine administration? Vaccine. 2008;26(26):3197–208.
19. Haq MI, Smith E, John DN, Kalavala M, Edwards C, Anstey A *et al.* Clinical administration of microneedles: skin puncture, pain and sensation. Biomed Microdev. 2009;11(1):35–47.
20. Gupta J, Felner EI, Prausnitz MR. Minimally invasive insulin delivery in subjects with type 1 diabetes using hollow microneedles. Diabetes Technol Ther. 2009;11(6):329–37. Erratum in: Diabetes Technol Ther. 11(7):471 (2009).
21. Huang J, D'Souza AJ, Alarcon JB, Mikszta JA, Ford BM, Ferriter MS *et al.* Protective immunity in mice achieved with dry powder formulation and alternative delivery of plague F1-V vaccine. Clin Vaccine Immunol. 2009;16(5):719–25.
22. Morefield GL, Tammariello RF, Purcell BK, Worsham PL, Chapman J, Smith LA *et al.* An alternative approach to combination vaccines: intradermal administration of isolated components for control of anthrax, botulism, plague and staphylococcal toxic shock. J Immune Based Ther Vaccines. 2008;6:5.
23. Alarcon JB, Hartley AW, Harvey NG, Mikszta JA. Preclinical evaluation of microneedle technology for intradermal delivery of influenza vaccines. Clin Vaccine Immunol. 2007;14(4):375–81.
24. Dean CH, Alarcon JB, Waterston AM, Draper K, Early R, Guirakhoo F *et al.* Cutaneous delivery of a live, attenuated chimeric flavivirus vaccine against Japanese encephalitis (ChimeriVax)-JE) in non-human primates. Hum Vaccin. 2005;1(3):106–11.
25. Mikszta JA, Sullivan VJ, Dean C, Waterston AW, Alarcon JB, Dekker JP *et al.* Protective immunization against inhalational anthrax: a comparison of minimally-invasive delivery platforms. J Infect Dis. 2005;191:278.
26. Mikszta JA, Dekker JP, Dean CH, Brittingham JM, Huang J, Sullivan VJ *et al.* Microneedle-based intradermal delivery of the anthrax recombinant protective antigen vaccine. Infect Immun. 2006;74:6806.
27. Beran J, Ambrozaitis A, Laiskonis A, Mickuviene N, Bacart P, Calozet Y *et al.* Intradermal influenza vaccination of healthy adults using a new microinjection system: a 3-year randomised controlled safety and immunogenicity trial. BMC Med. 2009;7:13.
28. Holland D, Booy R, De Looze F, Eizenberg P, McDonald J, Karrasch J *et al.* Intradermal influenza vaccine administered using a new microinjection system produces superior immunogenicity in elderly adults: a randomized controlled trial. J Infect Dis. 2008;198(5):650–8.
29. Leroux-Roels I, Vets E, Freese R, Seiberling M, Weber F, Salamand C *et al.* Seasonal influenza vaccine delivered by intradermal microinjection: a randomised controlled safety and immunogenicity trial in adults. Vaccine. 2008;26(51):6614–9.
30. Saville M, Marsh G, Hoffenbach A. Improving seasonal and pandemic influenza vaccines. Influenza Other Respi Viruses. 2008;2(6):229–35.
31. Intanza(R), The First Intradermal Influenza Vaccine, Receives The European Marketing Authorisation. http://www.medicalnewstoday.com/articles/140580.php (accessed 11/30/09), part of Medical News Today. http://www.medicalnewstoday.com/ (accessed 11/30/09).
32. Prausnitz MR, Mikszta JA, Raeder-Devens J. Microneedles. In: Smith EW, Maibach HI, editors. Percutaneous penetration enhancers. Boca Raton: CRC; 2006. p. 239–55.
33. Autret E, Guilloteau D, Corbel D, Jonville AP, Peyron R, Garrigue MA *et al.* Comparison of plasma concentration and tolerance of a single dose of human calcitonin by intradermal and subcutaneous administration. Therapie. 1991;46(1):5–8.
34. Kretsos K, Kasting GB. Dermal capillary clearance: physiology and modeling. Skin Pharmacol Physiol. 2005;18(2):55–74.
35. Bollinger A. Microlymphatics of human skin. Int J Microcirc Clin Exp. 1993;12(1):1–15.
36. Tripp CH, Haid B, Flacher V, Sixt M, Peter H, Farkas J *et al.* The lymph vessel network in mouse skin visualised with antibodies against the hyaluronan receptor LYVE-1. Immunobiology. 2008;213(9–10):715–28.
37. Segura E, Villadangos JA. Antigen presentation by dendritic cells *in vivo*. Curr Opin Immunol. 2009;21(1):105–10.
38. Zaba LC, Krueger JG, Lowes MA. Resident and "inflammatory" dendritic cells in human skin. J Invest Dermatol. 2009;129(2):302–8.

39. Laurent PE, Pettis R, Easterbrook W, Berube J. Evaluating new hypodermic and intradermal injection devices. Med Device Technol. 2006;17(2):16–9.
40. Lin S, Chen LL, Chien YW. Comparative pharmacokinetic and pharmacodynamics studies of human insulin and analogues in chronic diabetic Yucatan minipigs. J Pharmacol Exp Ther. 1998;286(2):959–66.
41. Naik A, Kalia YN, Guy RH. Transdermal drug delivery: overcoming the skin's barrier function. Pharm Sci Technol Today. 2000;3(9):318–26.
42. McAllister DV, Wang PM, Davis SP, Park JH, Canatella PJ, Allen MG *et al.* Microfabricated needles for transdermal delivery of macromolecules and nanoparticles: fabrication methods and transport studies. Proc Natl Acad Sci. 2003;100(24):13755–60.
43. Gin H, Hanaire-Broutin H. Reproducibility and variability in the action of injected insulin. Diabetes Metab. 2005;31(1):7–13.
44. Sindelka G, Heinemann L, Berger M, Frenck W, Chantelau E. Effect of insulin concentration, subcutaneous fat thickness and skin temperature on subcutaneous insulin absorption in healthy subjects. Diabetologia. 1994;37(4):377–80.
45. White HD, Ahmad AM, Vora JP. Effects of adult growth hormone deficiency and growth hormone replacement on circadian rhythmicity. Minerva Endocrinol. 2003;28(1):13–25.
46. Laursen T, Gravholt CH, Heickendorff L, Drustrup J, Kappelgaard AM, Jørgensen JO *et al.* Long-term effects of continuous subcutaneous infusion *versus* daily subcutaneous injections of growth hormone (GH) on the insulin-like growth factor system, insulin sensitivity, body composition, and bone and lipoprotein metabolism in GH-deficient adults. J Clin Endocrinol Metab. 2001;86(3):1222–8.
47. Kagan L, Gershkovich P, Mendelman A, Amsili S, Ezov N, Hoffman A. The role of the lymphatic system in subcutaneous absorption of macromolecules in the rat model. Eur J Pharm Biopharm. 2007;67(3):759–65.
48. Charman SA, McLennan DN, Edwards GA, Porter CJ. Lymphatic absorption is a significant contributor to the subcutaneous bioavailability of insulin in a sheep model. Pharm Res. 2001;18 (11):1620–6.
49. McLennan DN, Porter CJ, Charman SA. Subcutaneous drug delivery and the role of the lymphatics. Drug Discovery Today: Technologies. 2005;2(1):89–96.
50. Sharma R, Wang W, Rasmussen JC, Joshi A, Houston JP, Adams KE *et al.* Quantitative imaging of lymph function. Am J Physiol Heart Circ Physiol. 2007;292(6):H3109–3118.
51. Sevick-Muraca EM, Sharma R, Rasmussen JC, Marshall MV, Wendt JA, Pham HQ *et al.* Imaging of lymph flow in breast cancer patients after microdose administration of a near-infrared fluorophore: feasibility study. Radiology. 2008;246(3):734–41.
52. Søeborg T, Rasmussen CH, Mosekilde E, Colding-Jørgensen M. Absorption kinetics of insulin after subcutaneous administration. Eur J Pharm Sci. 2009;36(1):78–90.
53. Swartz M, Boardman K. The role of interstitial stress in lymphatic function and lymphangiogenesis. Ann NY Acad Sci. 2002;979:197–210.